

Reproductive strategy and embryonic development of *Bufotes surdus annulatus* in Iran

ZEINAB PARVARESH, NAZIHE SEDDIGHI, FATEMEH ROUSHENAS, SAMIRA RAHIMI, ELMIRA HASANI,
ZAHRA MOSSADEGHI & MOHSEN NOKHBATOLFOGHAHAI

Biology Department, Faculty of Sciences, Shiraz University, Shiraz, Iran

Corresponding author: MOHSEN NOKHBATOLFOGHAHAI, e-mail: nokhbeh@hotmail.com

Manuscript received: 13 October 2014

Accepted: 15 July 2015 by ARNE SCHULZE

Abstract. The reproductive strategy and embryonic development of *Bufotes surdus annulatus* from Fars Province, Iran, are described. Single stranded egg strings (clutch sizes 338–2019 eggs, mean 1032, $n = 69$) were generally laid in water-filled depressions in gravel near the edge of rivers. Eggs were 1.4 mm (± 0.18 mm) in diameter with jelly coats of 0.17 mm (± 0.04 mm). Hatching occurred at Gosner stages 17–18; features such as dental formula, external gills, cement gland, hatching gland, and external ciliation pattern are described and found to be similar but not identical to those found in *B. viridis*.

Key words. Amphibia, Anura, Bufonidae, larval morphology cement gland, clutch size, dental formula, external gills.

Introduction

The taxonomy of the toads of Iran is still unresolved. FROST (2014) lists *Bufotes* (previously *Pseudepidalea* and *Bufo*) *luristanicus* and *B. surdus*, noting that morphological evidence places *B. luristanicus* as a subspecies of *B. surdus* while molecular evidence suggests these are distinct species (JAVARI & TORKI 2009; FAKHARZADEH et al. 2014). Irrespective of this distinction, two subspecies of *B. surdus* have been identified: *B. s. annulatus* and *B. s. surdus* (SCHMIDTLER & SCHMIDTLER 1969, DUBOIS & BOUR 2010). *Bufotes surdus* BOULENGER, 1891 is a polytypic, small toad endemic to the west and south of Iran. In terms of occurrence, *B. luristanicus* has been found in the western Iranian provinces of Khuzestan and Lorestan in the western foothills of the Zagros Mountains (ANDERSON 1963, SCHMIDTLER & SCHMIDTLER 1969). *Bufotes s. surdus* has been recorded from the southern Iranian provinces of Sistan-o-Baluchistan, Kerman, and Hormozgan from 0 to 2,250 m a.s.l.. This subspecies has also been found in the Quetta region of Pakistan (SCHMIDTLER & SCHMIDTLER 1969, EISELT & SCHMIDTLER 1973). ZAREIAN et al. (2012) reported the existence of *B. surdus* in Kuh-e-Gorm, southwest of Jahrom, Fars Province, but there is doubt as to its being *B. s. surdus*. *Bufotes s. annulatus* has been reported only from Mahkuyeh, 80 km south of Shiraz, Fars Province at 1,400 m a.s.l. (SCHMIDTLER & SCHMIDTLER 1969). Surprisingly, there have been no further reports from the same or any other locations since

the initial collection of the one specimen of this subspecies.

In terms of morphological characters, SCHMIDTLER & SCHMIDTLER (1969) and BALOUCH & KAMI (1995) reported that the tympanic membrane was present in *B. luristanicus* and *B. s. annulatus*, but that it was very small and lying under the skin whereas no tympanic membrane is discernible in *B. s. surdus*. The three taxa seem to be particularly distinguished by the gradual reduction of tympanic membrane size along a west-to-east gradient in Iran and by the size of the parotoid glands. The IUCN (2014) assesses *Bufotes surdus* as a species of least concern, but notes that it may be a species complex and that its ecology is poorly known. The status of the populations recognized as subspecies have not been assessed and this is a particular issue for *B. s. annulatus*, which has not been reported on since SCHMIDTLER & SCHMIDTLER (1969) and EISELT & SCHMIDTLER (1973).

We located a breeding population of *Bufotes surdus annulatus*, with adults possessing all the features described by SCHMIDTLER & SCHMIDTLER (1969), at the village of Aliabad, Neyriz, in Fars Province, Iran. In order to further the knowledge on this subspecies, we here present data on reproductive, embryonic, and larval morphology, and development and adult morphometrics.

We compared the data on *Bufotes s. annulatus* to the data already available for *B. viridis*, the only other closely related bufonid species that is widely distributed in Fars Province.

Materials and methods

Bufo surdus annulatus spawn was collected from a site in Aliabad Village, Neyriz, in Fars Province. To the best of our knowledge and based on our preliminary studies across Fars Province, this site was the only suitable and accessible breeding site of this subspecies. The studied site (29°16'03.9" N, 54°13'58.2" E,) is located about 230 km southeast of Shiraz city, Fars Province, Iran, at an altitude of 1,795 m a.s.l. This site represents undisturbed natural habitat. The sampling location was along a seasonally dry river surrounded by mountains. Many springs from the mountains and ground drain into the river along its path. A number of pools have formed along the river's path, which is where the majority of samples were found, as well as from the margins of channels where the water current was slow (Fig. 1).

Spawn was collected from the edges of slow-current streams between March and April of 2013. Clutches were photographed with a digital camera in their natural condition. Twenty egg clutches were transferred to the laboratory and the rest were left in situ after being photographed. The clutches left in situ were labelled until the next observation and collection. We also collected larval specimens from nature. Observations of egg deposition sites were recorded and supported by photographs taken in situ. Clutches were subdivided and incubated in plastic containers (25 × 45 × 5 cm WLH) in the laboratory under identical conditions: photoperiod (12/12 h light/darkness), temperature (23.75 ± 0.16°C), pH (8.45), and number of specimens per litre of water. Each container held approximately three litres of water and 100 eggs. The containers were filled with dechlorinated tap water and aerated. Once the eggs hatched, the tadpoles at feeding stage were fed with boiled lettuce. Feeding frequency was initially once a day and 2–3 times a day once the larvae had grown sufficiently.

Embryos were staged using GOSNER'S (1960) (G) developmental table. For the embryonic study, 10 live embryos at each developmental stage were removed from the containers at specific times. Specimens for light-microscopic examina-



Figure 1. Habitat of *Bufo surdus annulatus* in Aliabad, Neyriz: Shallow river, ditches and pools beneath a rock are seen on the left of the photograph, taken on 4 November 2013.

tion were fixed in Bouin's fluid and those for scanning electron microscopy (SEM) were fixed in 2.5% glutaraldehyde in phosphate buffer. The time when more than half of the embryos of each clutch hatched was set as the hatching time, and the developmental stage at which the embryos emerged from the jelly coat was considered as the hatching stage.

The morphological stage at hatching was assessed by randomly selecting 30–40 of the newly hatched larvae from each clutch. To estimate the developmental stage in relation to time, we assumed the eggs had been fertilized at midnight of the night prior to the collection of fresh spawn. All Bouin's-fixed samples were transferred to 50% alcohol and then transferred to and kept in 70% alcohol for further examination.

Scanning Electron Microscopy (SEM) preparation and examination: Glutaraldehyde-fixed specimens for SEM were post-fixed in 1% osmium tetroxide, stained in 0.5% aqueous uranyl acetate, dehydrated in an acetone series, then critical-point dried, and coated with gold with a Polaron SC 515. They were then examined with a JSEM 6400 scanning electron microscope. Mouthparts, external gills, cement gland (CG), ciliated cells (CCs), and hatching gland cells (HGCs) were examined over a magnification range of 24–2000 × and captured with Image-slave for Windows (Meeco Holdings, Australia).

Paraffin wax sections: Histological studies were performed based on BANCROFT (1991) and GURR (1962) methods, including the preparation of cross sections of the external gill region. To do this, samples at stage G22 dissected from the head region were isolated under a stereomicroscope and then fixed in Bouin's solution. The samples were dehydrated in an ethanol series, cleared in xylol, embedded in paraffin wax, cut at 5–7 μm and then stained by H&E. The microscopic slides were examined over a range of magnifications.

Clutch parameters, including the number of eggs in each clutch (clutch size) and egg diameter, were measured. The eggs in each clutch were counted immediately after transferring *Bufo surdus annulatus* spawn to the laboratory and before fixation. The data obtained from the photographs taken of the clutches in nature were also included in the mean clutch size calculation. Thirty-three fixed eggs from each clutch were chosen from the first day of development at a stage prior to G10 – when embryos are still spherical – to measure the mean diameter of the eggs and the thickness of their jelly coats. A graticule with an accuracy of 50 μm was used to measure the egg diameter and the thickness of the surrounding jelly.

From the 20 clutches that we used in this study, body length (BL), total length (TL) and tail length (TAL) were measured in a series of embryos and larvae stored in 70% alcohol (5–6 samples were fixed in each stage for each clutch). Fixation and measurement processes were started from stage G17 (tail bud stage) and continued until stage G25. Size at age of embryos and larvae was calculated by measuring the average change in the lengths of larvae at different times. Developmental stage at age of embryos and larvae was also calculated by measuring the different developmental stages at various points of time.

Due to difficulties in rearing the growing tadpoles to more advanced stages in an aquarium, biometry data were obtained from larvae that were captured in nature at stages G26 to G28, G31, G34, G38, and G41 ($n = 15$ at each stage). Based on McDIARMID & ALTIG (1999), we measured tadpole total length (TL), body length (BL), interorbital distance (IOD), internarial distance (IND), tail length (TAL), tail muscle width at the base of the tail (TMW), tail muscle depth at the base of the tail (TMD), maximum dorsal tail fin depth (MDFH), and maximum ventral tail fin depth (MVFH).

Morphological assessment of embryonic and larval organs

External gills: The development of the external gills was assessed from stages G17/18 to G25 by SEM photographs and also from fixed samples using a dissecting microscope. We assessed the position of the gills, the number of branches, and the number of secondary filaments on each side at stage G22 when the external gill was developed to the maximum (in total 20 clutches; 15 samples were examined from each clutch).

Cement gland (CG): The developmental pattern of the CG was studied from stage G15/16 to stage G26 by both SEM photographs and dissecting microscope (10 samples at each stage).

Ciliated cells (CCs): Distribution and density of the CCs at each stage were examined where SEM photographs were available. We assessed the presence/absence and density of CCs at different locations on the body surface of embryos/larvae: nostrils, CG, external gills, ventral and lateral sides of the head, ventral and lateral sides of the trunk, as well as the tail surface. Ciliated cell density, based on the ratio of areas with CCs to areas with no CCs, was classified into five categories: 1. Very dense: the ratio of areas with CCs to those with none is between 3:1 and 1:0, meaning that there is no space between CCs (*****); 2. Dense: the ratio is between 3:1 and 2:1 (****); 3. Intermediate: the ratio is between 2:1 and 1:2 (***); 4. Scattered: the ratio is less than 1:2 and 1:3 (**); 5. Sparse: the ratio is less than 1:3 (*).

Hatching gland cells (HGCs): SEM photographs at low and high magnification were taken from the dorsal side of the head and trunk of embryos and larvae with focus on the HGCs (examining the areas where HGCs are expected to be observed). The stages when the HGCs appeared or disappeared on the surface were distinguished. The stage when the HGCs were close together and highest in number was also recorded.

Dental formula

In order to identify the dental formula of *Bufo surdus annulatus*, 15 samples from each clutch at stage G26, the earliest stage at which tooth rows are well developed according

to McDIARMID & ALTIG (1999) and 5 samples at stage G41 were randomly chosen from lab-reared tadpoles as well as from wild-caught ones. The number of tooth rows on the anterior and posterior labium were counted and any gaps noted using the formula recommended by McDIARMID & ALTIG (1999).

Adults (amplectant pairs and single males) were collected and transferred to the laboratory for verification of their specific identity and examination of their biometrics. Identification was based on the description by SCHMIDTLER & SCHMIDTLER (1969). Adults were kept in a vivarium and fed with fruitflies. Adults were weighed after removal of any surface moisture with an accuracy of 0.01 g. After completion of measurements, these adults were lethally anaesthetized with ether and fixed in Bouin's fluid for further examination.

Biometric characteristics of adult toads (9 males, 5 females) were measured based on the characters presented in BALLETO et al. (1985). All measurements were made using a calliper with an accuracy of 0.01 mm. Other morphological characters including the shape and colour of spots on the surface and the positions of the parotoid glands and tympani were also recorded.

Biometric characters and weights of adult males and females were compared and analysed by an independent one-sample t-test at 5% level of significance using SPSS version 16.

Results

Spawning period

It can be concluded from our first observation of fresh egg clutches with no later stages (embryos or larvae) in the field that *Bufo surdus annulatus* started spawning on 11 April in 2013. Furthermore, since no fresh eggs were observed on 18 May and the youngest larval samples present were at G23 (i.e., approximately one week after the last spawning event), the *B. s. annulatus* spawning season possibly finished on 10 May in 2013. Therefore, the spawning period and annual breeding season of this species is estimated at lasting about 4 weeks.

Egg clutch locations and sizes

Nearly all *Bufo surdus annulatus* egg strings were found as single strands in stagnant water (Fig. 2). In some cases, two strings were found close together: We supposed that these were part of the same clutch and counted them together. In some cases, a continuous strand was linked to such coiled strings. All clutches were located in water-filled depressions in gravel at the edge or just beyond the edge of the stream. These depressions were almost circular and ranged from 15–25 cm in diameter (Fig. 2). The mean clutch size (\pm SD; $n = 69$) was $1,031.5 \pm 426.2$. Eggs ($n = 45$) had a mean (\pm SD) diameter of 1.4 ± 0.18 mm with jelly coats 0.17 ± 0.04 mm thick (Table 1).

Embryonic development of *Bufoes surdus annulatus*

Table 1. Clutch and egg parameters of *Bufoes surdus annulatus*; G – Gosner stage.

Clutch and egg parameters	Number of clutches/eggs examined	Minimum	Maximum	Mean±SD
Clutch size	69 clutches	338 eggs	2019 eggs	1031.5±426.2
Hatching stage	20 clutches	G17	G18	17.3±0.4
Hatching time	20 clutches	65 hrs	78 hrs	72.95±4.7 hrs
Total egg diameter (egg + jelly coat)	45 eggs	1.5 mm	1.95 mm	1.61±0.22 mm
Egg diameter	45 eggs	1.2 mm	1.8 mm	1.45±0.18
Jelly coat thickness	45 eggs	0.15 mm	0.35 mm	0.17±0.04

Early development

Early development followed the pattern that is normal for anuran eggs with unequal holoblastic cleavage (GOSNER

1960). Hatching occurred at stages G17–18 after incubation under laboratory conditions in water at $19.2 \pm 1.3^\circ\text{C}$ for 73.0 ± 4.7 h (n = 100). The progression in developmental stages was directly correlated with time in a linear pattern



Figure 2. *Bufoes surdus annulatus* spawn at low and high magnifications (A–C) and *Bufoes viridis* spawn (D) at high magnification. A) The arrow points out the rim of a circular nest in gravel. Spawn in the centre of the nest. B) Spawn from Fig. A shows as being single-stranded under magnification. C) Two separate batches of eggs in continuous strands. D) Double-stranded *Bufoes viridis* spawn (courtesy of BADPAYMAN-JAHROMI 2008).

(Fig. 3A). Figure 3B shows the relationship between total length of embryos and larvae and developmental time. The relationship between time and body length shows a sigmoid pattern from stage G13 up to stage G24, the last stage studied.

Tadpole morphology

We experienced difficulty with rearing tadpoles in the laboratory with more than 90% dying after reaching stage G25. Our description of the tadpoles is therefore based on post-stage G25 specimens captured in the field.

Figure 4 shows light-microscopic photographs of larvae at stages G26 and G41. At stage G26, BL is about 40% of TAL; the tail has a rounded tip with dorsal and ventral tail

fins being unpigmented and approximately of equal height. Body and tail axis are black in colour. The eyes are dorsolaterally positioned. The spiracle is a single midlateral opening on the left side of body (sinistral). The tadpole has a medial vent tube. The tadpole at stage G26 is 12.3 mm long and 42.5 mm long on average at stage G41, just before the start of metamorphosis.

Larvae at stage G26 and G41 were used for identifying the dental formula. The larva has an oral disc with two rows of teeth on the upper lip (anterior labium) with a gap in the second row, and three undivided rows of teeth on the lower lip (posterior labium). Therefore, the dental formula of the larva is $2(2)/3$ (Fig. 5). Table 2 shows the results of the biometrics of eight characteristics of *Bufoles surdus annulatus* larvae at different developmental stages between G26 and G41.

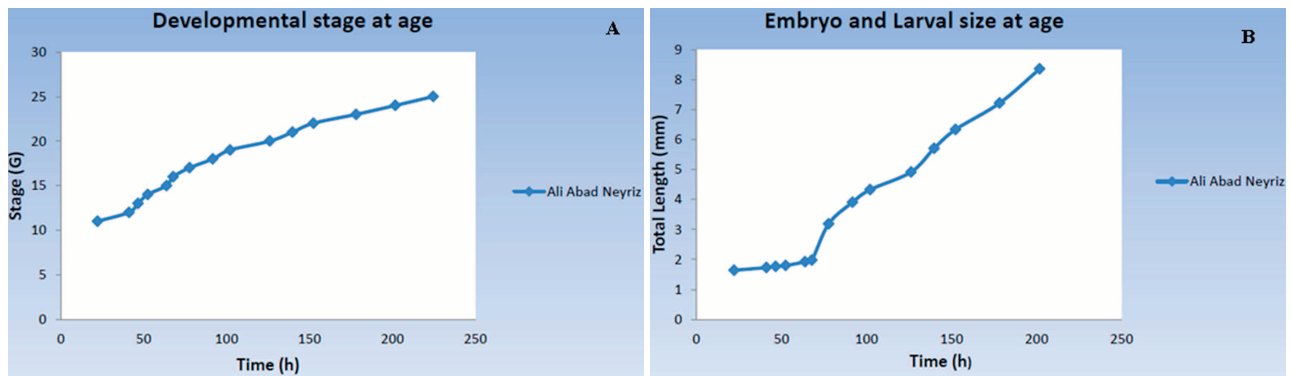


Figure 3. Diagrams of developmental and growth patterns in *Bufoles surdus annulatus* larvae. A) developmental stage at age; B) size at age based on total length of embryos and larvae.

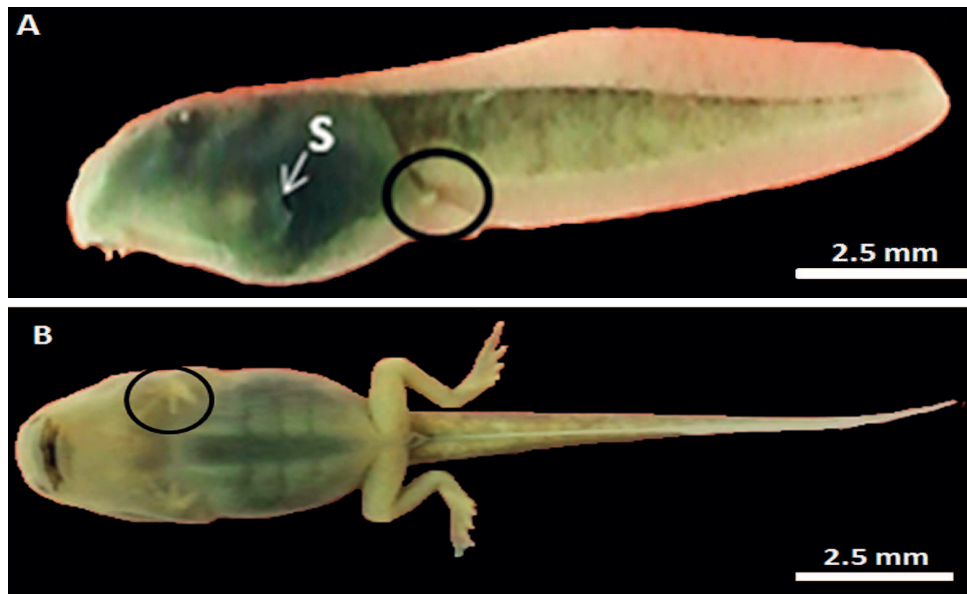


Figure 4. Light-microscopic photographs of the external morphology of growing larvae of *Bufoles surdus annulatus* at stages G26 and G41. A) lateral view of a tadpole at stage G26 showing the early stage of leg bud (black circle); B) ventral view of a tadpole at stage G41 with well-developed hands being visible under the transparent skin (black circle); S – spiracle.

Table 2. Biometrics at seven developmental stages of larvae of *Bufores surdus annulatus*; body length (BL); tail length (TAL); total length (TL); tail muscle height (TMH); maximum tail height (MTH); tail muscle width (TMW); interorbital distance (IOD); inter-narial distance (IND).

Stage	BL	TAL	TL	TMH	MTH	TMW	IOD	IND
26	4.5±0.25	7.84±0.8	12.34±1.01	0.9±0.13	1.85±0.09	0.63±0.047	1.27±0.15	0.64±0.08
27	7.08±0.41	12.69±0.92	19.78±1.29	1.7±0.22	3.14±0.2	1.17±0.13	2.14±0.14	1.15±0.08
28	8.22±0.49	14.03±1.27	22.25±1.57	2±0.24	3.96±0.35	1.47±0.16	2.48±0.23	1.35±0.14
31	11.78±0.87	20.25±1.78	32.03±2.38	3.04±0.27	5.26±0.6	2.21±0.19	3.49±0.22	1.81±0.21
34	14.39±0.88	25.71±1.8	40.10±2.46	4.15±0.22	6.05±0.6	2.99±0.2	3.97±0.12	2.13±0.4
38	17±0.43	29.37±1.97	46.38±2.25	4.8±0.42	6.64±0.52	3.67±0.26	4.72±0.24	2.23±0.28
41	14.85±0.78	27.61±1.2	42.47±1.88	4.27±0.26	6.17±0.51	3.15±0.24	4.65±0.1	1.9±0.18

Ultra-structural studies of external organs in *Bufores surdus annulatus* embryos and larvae

Morphology and developmental pattern of external gills: The external gills of *Bufores s. annulatus* embryos and larvae appeared as two bulges on both sides of the head at stage G18 and reached the peak of development at stage G22. These structures were then gradually covered by the operculum and disappeared at stage G25 (Fig. 6). The larvae have short external gills with three main stalks on either side of the head; tissue sections of external gills reveal three main stems on each side resulting in a total of nine filaments on each side of the head. The mean maximum length of filament at stage G22 was $286.3 \pm 7.7 \mu\text{m}$ ($n = 5$).

Morphology and developmental pattern of CG: Cement glands appeared at stage G15/16 and disappeared at stage G26 from the ventral side of the head. The two parts of the CG initially formed a wide U- and then a V-shaped groove (Fig. 7A). The two arms of the V at the base of the

gland later disconnected, and the whole gland became M-shaped (Fig. 7B); then the two arms separated to assume almost the shape of an elongated horseshoe (Fig. 7C). The groove then slowly disappeared and the two arms became flattened and retained the shape of two rods (Figs 7D–E) before disappearing at stage G26 (Fig. 7F).

Distribution of CCs and HGCs on the surface of embryos and larvae

Table 3 details the CC pattern of *Bufores surdus annulatus*. Ciliated cell density at stage G17 (the earliest stage examined) was dense to very dense in most parts of the embryo. Ciliated cells remained on most areas of the body at stage G26, the latest stage we examined, but at low densities. Ciliated cells on the CG and the ventral side of the head were very dense from stage G17 to G19. The maximum density of CCs on the body surface occurred at stages G17 and G18. Ciliated cell density remained dense around the nostril up to stage G24 and then intermediate at least up to stage G26, the last stage examined (Figs 8A–B). Hatching gland cells were identifiable by their dense clusters of microvilli. Maximum extension and a continuous patch or line of HGCs were observed at stage G17, with no other cells intervening on the top of the head. The hatching gland regressed and the cells became smaller and separated from each other at later stages (Figs 8C–D).

Morphometrical analysis of adults

Table 4 shows 21 biometric characteristics of *Bufores surdus annulatus* adults separated by sex. Independent one-sample t-test showed that mean length ($48.31 \pm 2.63 \text{ mm}$) was significantly ($P < 0.017$; $df = 12$; $t = -2.764$; $F = 0.002$) greater in females than in males (43.97 ± 2.9). Interorbital distance ($P < 0.031$; $df = 12$; $t = 2.436$; $F = 0.392$), width of upper eyelid ($P < 0.047$; $df = 12$; $t = -2.211$; $F = 0.684$), and length of the first finger of the hand ($P < 0.002$; $df = 12$; $t = -3.807$; $F = 1.567$) were also found to be significantly different between males and females. Mean weight ($9.48 \pm 2.05 \text{ g}$) was significantly ($P < 0.025$; $df = 12$; $t = -2.570$; $F = 0.037$) greater in females than in males ($6.89 \pm 1.67 \text{ g}$). Dark olive ring-shaped spots were arranged on the back (Fig. 9), and the tympanum

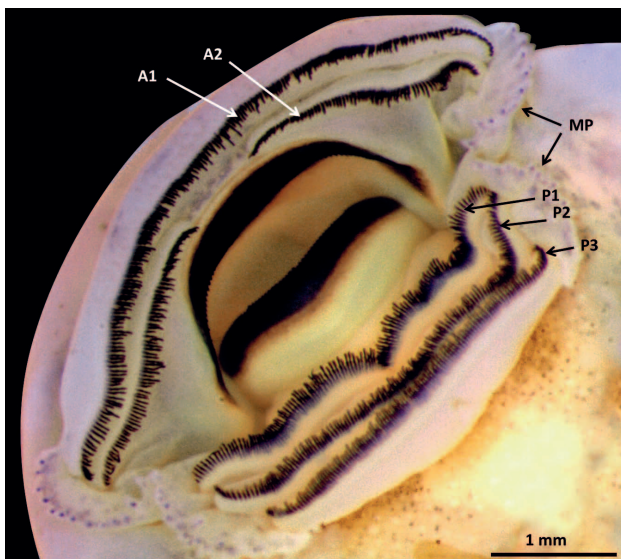


Figure 5. Oral disc of a *Bufores surdus annulatus* tadpole at stage 41, illustrating the general organization of the oral apparatus. A1 and A2 – first and second anterior tooth rows; MP – marginal papillae; P1, P2, and P3 – first, second and third posterior tooth rows.

Table 3. Ciliated cell distribution and density in *Bufo sardus annulatus*; Key: * – sparse; ** – scattered; *** – intermediate dense; **** – dense; ***** – very dense; d – structure regressed or covered; p – structure not yet developed.

Stage	Lateral side of head	Ventral side of head	Ventral side of trunk	Lateral side of trunk	Tail	Nostril	External gill	Cement gland
17	***	****	***/**	***	***	***	p	****
18	***	****	***/**	***	***	***	**	****
19	**	****	***/**	***	***	***	**	****
21/22	**	***	***/**	***	**	***	*	****
23	**	***/**	***/**	***	**	***	*	***
24	*	**	**	**	**	***	*	**
25	*	**	**	**	**	**	d	*
26	*	**	**/*	**	*	**	d	d

was almost hidden under the skin and appeared very small ($1/5$ of horizontal diameter of the eye) on the surface.

Discussion

According to the morphological characteristics and studied traits, the toad we studied was *Bufo sardus annulatus*, a specimen of which was previously found 5 km north of Mahkuyeh, 80 km south of Shiraz in 1969 (SCHMIDTLER & SCHMIDTLER 1969), and now for the first time in the Aliabad region, 230 km southeast of Shiraz. Study of the subspecies in its habitat yielded considerable information about its environment, reproductive mode including spawning, clutch size, spawning time, and breeding season, and revealed interesting differences to other toads including *B. viridis*, the closest related species in Fars Province, for which detailed reproductive, embryonic, and adult information was available in our databank (BADPAYMAN-JAHROMI et al. 2015 unpubl. data). Based on our observations of egg clutches in the field we concluded that the spawning period and annual breeding season of *B. s. annulatus* lasts approximately one month, which is very short compared to that of *B. viridis* in the region (spawning period lasting from February to June [NOKHBATOLFOGHAI 2009, ROUSHENAS 2013]). The restricted spawning location of *B. s. annulatus* (only found in a very limited area of Aliabad and reported from Mahkuyeh) and the short breeding season highlight the importance of studying and protecting this subspecies. The results suggest that spawning requires particular ecological conditions, as is emphasized by the facts that the amplexant adults did not successfully spawn under laboratory conditions and we had difficulty rearing the tadpoles to more advanced developmental stages in the laboratory. The reason for the high mortality rate was not fully clear, as later-stage tadpoles captured from nature lived on for many days in the lab. One explanation could be that they have very specific dietary needs. The later-stage tadpoles captured from nature were maintained with water and food (algae) brought from their natural habitat (pools).

The maximum number of eggs in one clutch was about 2000; in Iranian green toads, *Bufo viridis*, (female

SVL = 70.4 ± 6.02 mm), clutch size averaged more than 7,000 and in some cases numbered more than 9,000 eggs (NOKHBATOLFOGHAI 2009). SMITH & FRETWELL (1974) found that in amphibians, larger females have larger egg clutches and larger eggs, because they have larger storage capacities and can expend more energy on reproduction. It was therefore expected that *B. sardus annulatus*, with its small body size (female SVL = 48.31 ± 2.63 mm), would have a smaller clutch size. The reason for producing double-stranded spawn in almost all toads is to allow the string of eggs to pass through each oviduct and be released from the cloaca simultaneously. Producing a single strand of eggs in *B. s. annulatus* probably demonstrates that the female uses only one of the oviducts at a time or releases the eggs from her oviducts one after the other. The latter reasoning could be supported by our observing spawn in two patches (Fig. 2C), indicating that females laid their eggs in two processes that each produced a patch of spawn from one oviduct. Further investigation is needed to corroborate this ovulation and spawning procedure.

HADDAD & PRADO (2005) differentiated 39 reproductive modes in amphibians. Using a natural or artificial water-filled basin adjacent to a pond or stream for the deposition of eggs (mode 4) has so far been reported only for some hylids. In general, bufonids simply wrap their egg strings around vegetation in ponds. We know of no previous report of a bufonid depositing its eggs in a water-filled basin. We cannot be sure whether the toads actually constructed the basins or used natural ones as we were not able to observe the complete sequence of mating behaviour.

External gills: The larvae have external gills with three main stalks on either side of the head and nine filaments in total on each side. BADPAYMAN (2008) found the same number of filaments on each side in *Bufo viridis* (nine), but four main branches of the external gill on each side when they studied four different populations, which is therefore different from *B. s. annulatus*. The maximum sizes of the filaments in both species showed the external gill to be poorly developed compared to some other species (NOKHBATOLFOGHAI & DOWNIE 2008). NOKHBATOLFOGHAI & DOWNIE (2008) found differences in the histological structure of external gill filaments in different

species and variation in the number and size of filaments between different individuals of a species. We found consistency and no differences among individuals in terms of the number of filaments in *B. surdus annulatus*.

Cement gland: The CG in *Bufoles surdus annulatus* appeared at G14 and became U-shaped at G15. The shape of the gland changed to M-shaped during hatching, and split

into two parts at G19, which is similar to type A in *Rhinella beebei* (NOKHBATOLFOGHAHAI & DOWNIE 2005). The second half of CG development showed by the two elongated horseshoe and narrow shapes of CGs, which is similar to type B in *B. viridis* and two other species in the list of bufonid species studied by NOKHBATOLFOGHAHAI & DOWNIE (2005). This categorization was based on five developmen-

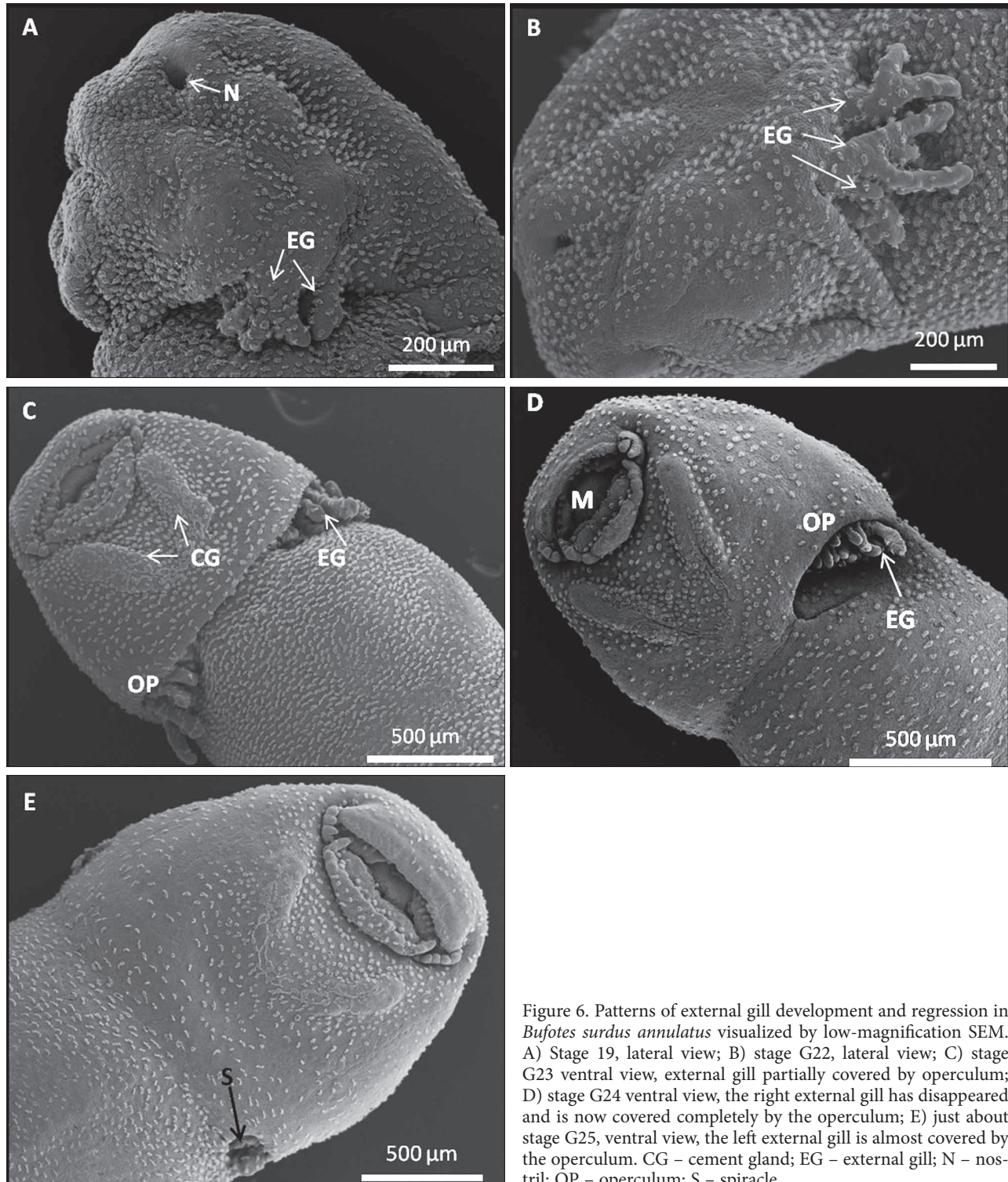


Figure 6. Patterns of external gill development and regression in *Bufoles surdus annulatus* visualized by low-magnification SEM. A) Stage 19, lateral view; B) stage G22, lateral view; C) stage G23 ventral view, external gill partially covered by operculum; D) stage G24 ventral view, the right external gill has disappeared and is now covered completely by the operculum; E) just about stage G25, ventral view, the left external gill is almost covered by the operculum. CG – cement gland; EG – external gill; N – nostril; OP – operculum; S – spiracle.

tal pattern types (A–D) introduced by NOKHBATOLFOGHAI & DOWNIE (2005). Therefore the CG developmental pattern in *B. s. annulatus* is typical of bufonids and partially overlaps the pattern of gland development in *B. viridis*.

In both species, CCs are very dense on the CG, and the gland disappears at stage G26.

Ciliated cells and HGCs: The ciliary cell patterns on the surface of *Bufoetes surdus annulatus* embryos and larvae

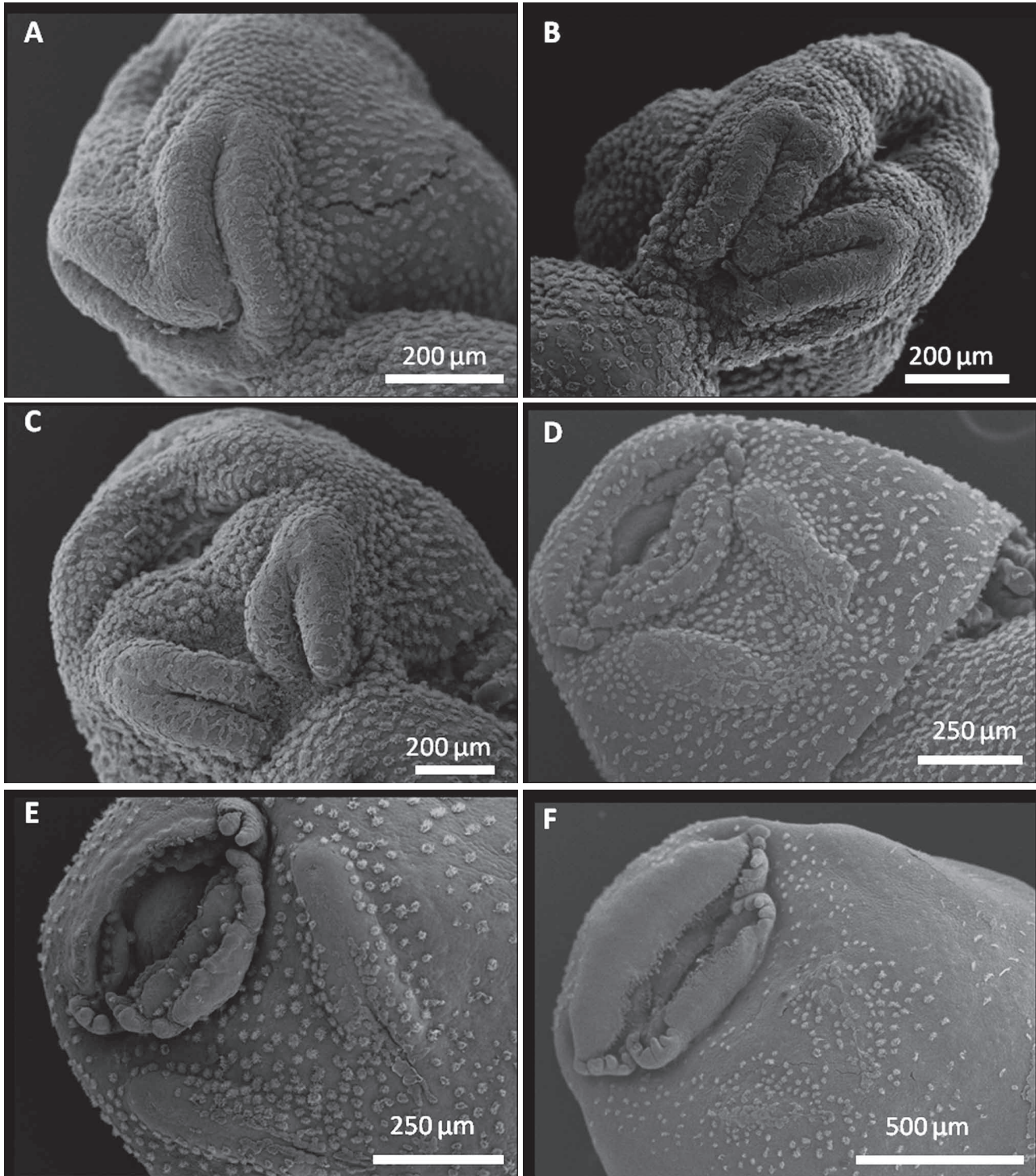


Figure 7. Patterns of cement gland development and regression in *Bufoetes surdus annulatus*, ventral views, visualized by low-magnification SEM. A–B) stages G17 and G18, respectively. The V-shaped groove flattens to a U, with the whole gland being M-shaped. C) stage G21, the two arms have separated to form almost horseshoe-shaped structures. D–E) stages G23 and G24, respectively, showing that the grooves slowly disappear. F) stage G26, the cement glands have almost disappeared.

Embryonic development of *Bufo surdus annulatus*

Table 4. Twenty-one biometric characters of adult *Bufo surdus annulatus* separated by sex (total n = 14; 9 males, 5 females; all measurements in mm); df for all characters was 12; * = Significance of differences between males and females P < 0.05.

Character	Sex	Mean	Maximum	Minimum	p	t	f
Snout to urostyle*	Female	48.31±2.63	51.61	45.41	0.017	-2.764	0.002
	Male	43.97±2.9	49.30	39.52			
	Total	45.52±3.45	51.61	39.52			
Width of head	Female	15.90±1.23	17.37	14.20	0.41	-0.838	0.025
	Male	15.27±1.38	18.36	14			
	Total	15.50±1.31	18.36	14			
Length of head	Female	14.95±1.22	15.69	12.78	0.51	0.674	0.006
	Male	15.40±1.18	17.20	13.57			
	Total	15.24±1.17	17.20	12.78			
Internarial distance	Female	3.31±0.44	3.86	2.66	0.91	-0.110	0.197
	Male	3.29±0.3	3.73	3.01			
	Total	3.30±0.34	3.86	2.66			
Interorbital distance*	Female	3.34±0.32	3.67	2.86	0.031	2.436	0.392
	Male	3.87±0.42	4.69	3.26			
	Total	3.68±0.46	4.69	2.86			
Width of upper eyelid*	Female	4.30±0.53	4.92	3.56	0.047	-2.211	0.684
	Male	3.77±0.37	4.40	3.17			
	Total	3.96±0.49	4.92	3.17			
Vertical diameter of tympanum	Female	4.75±0.71	5.38	3.55	0.147	-1.550	0.214
	Male	4.12±0.74	5.59	3.45			
	Total	4.34±0.77	5.59	3.45			
Horizontal diameter of eye	Female	5.66±0.52	6.55	5.25	0.23	-1.261	0.008
	Male	5.29±0.53	6.47	4.60			
	Total	5.42±0.54	6.55	4.60			
Minimum distance from nostril to anterior corner of eye	Female	4.67±0.75	5.35	3.73	0.3	1.078	0.21
	Male	5.16±0.84	6.20	3.48			
	Total	4.98±0.81	6.20	3.48			
Minimum distance from nostril to tip of snout	Female	1.36±0.39	1.36	0.84	0.56	0.594	3.679
	Male	1.45±0.2	1.83	1.11			
	Total	1.42±0.27	1.83	0.84			
Length of arm to wrist	Female	14.82±1.72	16.93	12.15	0.34	0.978	1.368
	Male	16.07±2.52	20.77	13.25			
	Total	15.62±2.28	20.77	12.15			
Length of hand	Female	10.82±1.59	12.78	8.50	0.94	-0.071	0.197
	Male	10.76±1.33	13.55	9.49			
	Total	10.78±1.37	13.55	8.50			
Width of first finger of hand	Female	2.17±0.43	2.84	1.68	0.97	-0.027	0.892
	Male	2.16±0.74	3.77	1.42			
	Total	2.16±0.62	3.77	1.42			
Length of first finger* of hand	Female	5.77±0.67	6.46	4.76	0.002	-3.807	1.567
	Male	4.65±0.43	5.34	3.98			
	Total	5.05±0.75	6.46	3.98			
Length of hind limb to tibiotarsal articulation	Female	33.39±2.34	37.25	31.59	0.76	0.301	0.083
	Male	33.74±1.92	36.12	31.22			
	Total	33.62±2	37.25	31.22			
Length of tarsus	Female	9.39±0.5	9.99	8.76	0.2	1.342	1.952
	Male	10.29±1.42	13.48	8.75			
	Total	9.97±1.23	13.48	8.75			
Length of metatarsal tubercle(s)	Female	2.12±0.38	2.68	1.61	0.19	1.379	0.536
	Male	2.34±0.22	2.64	1.97			
	Total	2.26±0.29	2.68	1.61			

Character	Sex	Mean	Maximum	Minimum	p	t	f
Webbing	Female	10.81±0.432	11.20	10.16	0.55	0.611	2.915
	Male	11.03±.82	12.10	9.61			
	Total	10.95±0.69	12.10	9.61			
Length of foot	Female	20.54±.55	22.80	18.73	0.48	-0.729	0.601
	Male	20.011±1.16	21.44	17.43			
	Total	20.20±1.28	22.80	17.43			
Minimum distance from eye to tympanum	Female	1.27±.19	1.50	0.97	0.68	0.414	3.230
	Male	1.35±0.4	1.86	0.7			
	Total	1.32±0.33	1.86	0.7			
Elongation of mandible	Female	13.18±2.71	17.56	10.86	0.19	-1.361	1.381
	Male	11.63±1.69	15.53	9.34			
	Total	12.18±2.14	17.56	9.34			

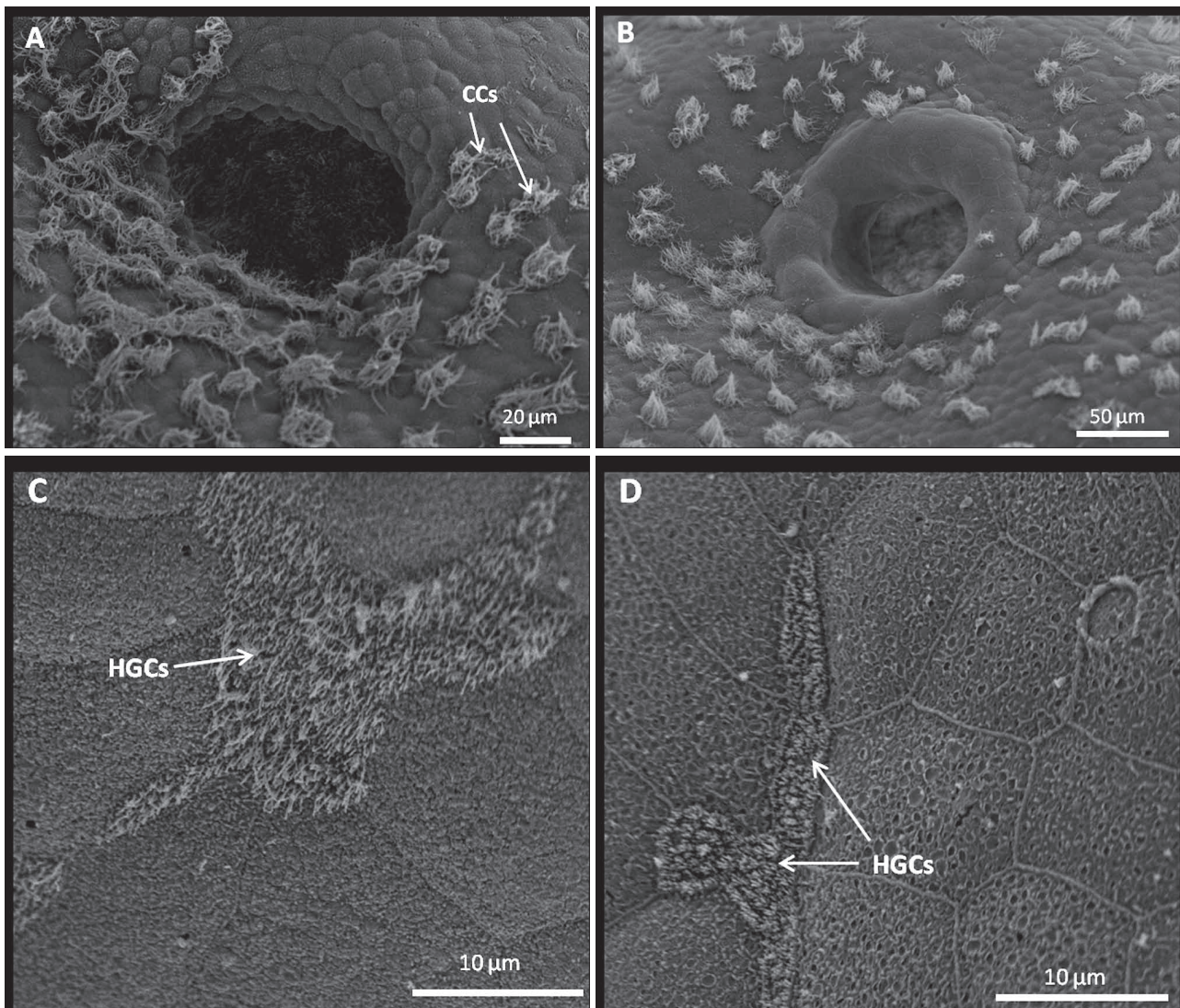


Figure 8. High-resolution SEM micrograph A) Nostril at stage G24 showing the dense ciliated cell pattern around the pore; B) Nostril at stage G26 with an intermediate ciliated cell pattern around the prominent edge of the pore; C) Hatching gland cells at stage G17, showing the wide patch of highly microvillated cells; D) Hatching gland cells at stage G24 with the area of the gland and the size of microvillated cells reduced. CCs – Ciliated cells; HGCs – Hatching gland cells.

especially around the nostril, external gills, CG, and ventral side of the head were very similar to those reported by NOKHBATOLFOGHAI et al. (2005) for *B. viridis*. Hatching gland cells showed a pattern regarding shape (elongated cells) and distribution (dorsal side of the head and extending to the back of the trunk) that is similar to *B. viridis*. In both species, the HGCs can be clearly seen at later stages (G24). The role of HGCs at hatching stage (G17/18) is clear, but its persistence until later stages may suggest other roles for these specialized cells as well (NOKHBATOLFOGHAI & DOWNIE 2007).

We have no record of larval morphology and biometrics from past reports of *B. s. annulatus*: all characters we measured increased in size from stage G26 to stage G38. The size of the tail was reduced during stage G41 due to the start of metamorphosis and tail resorption. Reduction in trunk (body) length may be a consequence of the shortening of the intestine during metamorphosis. Other characters shrinking in size include the distance between the sensory organs of the head, including nares and eyes, due to the changing shape of the head and the convergence of the location of the paired sensory organs to their permanent positions.

Dental formulae vary with the species of anurans (JENNINGS & SCOTT 1993, KHAN & MUFTI 1994) and this trait can be used to some extent for species identification, although intraspecific variations were seen in the number of

dental rows between different populations of some species (MCDIARMID & ALTIG 1999, AMANAT-BEHBAHANI et al. 2014). In cases where the numbers of dental rows are identical, variation is reported due to the presence or absence of gaps in tooth rows. The oral disc of all *Bufo surdus annulatus* larvae examined at G26 (when dental rows were completed) and G41 had a similar dental formula with two tooth rows on the upper lip, a median gap in the second row, and three continuous rows of teeth on the lower lip. Thus, the dental formula of the larvae of this subspecies exhibited no individual variability. We compared the dental formula between larvae reared in the lab and those captured from a wild habitat and no differences were observed. This finding demonstrated that environment and the type of food do not affect – at least during a short period – the shape of oral tooth rows. The dental formula identified is exactly the same as the one BADPAYMAN-JAHROMI (2008) found in different populations of *B. viridis* in Fars Province, Iran.

SCHMIDTLER & SCHMIDTLER (1969) reported only on the singular holotypic semi-adult male specimen of *Bufo s. annulatus* (SVL = 37 mm). Although all the characters they identified on this adult are compatible with our adult specimens, the total length of the holotype is less than both our mean female length (48.31 ± 2.63 mm) and mean male length (43.97 ± 2.9). We consider our specimens to be adults, as we collected them in amplexus next to their spawn.

Bufo surdus annulatus was found in an upland riverine habitat surrounded by mountains with waterfalls and small ponds and tunnels. Adults were found in large cracks in rocks or crevices in tree trunks. Juveniles were found in separated and isolated pools with depths of about 20 to 50 cm. *Pelophylax ridibunda* were observed in pools and streams but far from the microhabitat of *B. s. annulatus* juveniles. Habitat characterisations of adult *B. s. annulatus*, *B. s. surdus*, and *B. luristanicus* show that the populations of all three taxa live in mountain stream habitats (*B. luristanicus*, 350–500 m a.s.l.; *B. surdus surdus*, 1,100 m a.s.l.; *B. s. annulatus*, 1,795 m a.s.l.). The holotype of *B. s. annulatus* from Mahkuyeh was also found at 1,400 m. a.s.l. While details of spawning microhabitat as well as embryonic and larval development of *B. s. annulatus* are reported here, there appears to be no such information on the two other taxa. Although several studies including those on adult biometrics and karyotype (STÖCK et al. 2001, FAKHARZADEH et al. 2014) have been conducted to interpret the phylogeny of these three taxa, the study of reproductive strategies and embryonic development can be very helpful for *B. s. surdus* and *B. luristanicus* to characterise these taxa more comprehensively.

Bufo s. annulatus from Fars Province was studied in order to fully describe the subspecies and investigate its embryonic and larval developmental stages and the reproductive strategy of adults. *Bufo s. annulatus* was identified by some key morphological traits, including olive-green circular spots on the back of the body, a distance between the eyes that is larger than the length of the upper eyelid, and the presence of a very small tympanum concealed



Figure 9. Light-microscopic photograph of a young *Bufo surdus annulatus* (male) in dorsal view showing the dark olive ring-spots scattered on the body.

under skin. Females produce eggs in single long strands deposited in a gravel nest. Hatching stage, HGC and CC patterns and distribution and dental formula (2(2)/3) are similar to *B. viridis*. Cement gland developmental pattern was a sequential mix of types A and B, which is not exactly identical to the CG developmental pattern in *B. viridis*. The number of branches in the external gill is three and therefore different from the four branches in *B. viridis*. Study on the developmental patterns and reproductive strategies of the two other subspecies *B. s. surdus* and *B. luristanicus* are highly recommended to find out if there are any similarities and differences between these subspecies. Developmental study is important to help taxonomists assess subspecies and species more completely.

Acknowledgements

The authors thank ROGER DOWNIE from Glasgow University for his reviewing our draft manuscript, MARGARET MULLIN for help with the processing of SEM samples and giving technical advice, and SOHEILA JAVANMARDI and YASER BAKHSI for their help during fieldwork. We also thank the Department of Biology of Shiraz University for financial support and the Faculty of Agriculture of Shiraz University for help with sampling.

References

- AMANAT-BEHBAHANI, M., M. NOKHBATOLFOGHAI & H. R. ESMAEILI (2014): Intraspecific variation in *Pelophylax ridibunda* (*Rana ridibunda*) in Southern Iran: life history and developmental patterns. – Iranian Journal of Animal Biosystematics, **10**: 11–28.
- ANDERSON, S. C. (1963): Amphibians and reptiles from Iran. – Proceedings of the California Academy of Sciences, San Francisco, **31**: 417–498.
- BADPAYMAN-JAHROMI, M. (2008): A comparative study of embryonic and larval development, also adult form in four populations of *Bufo viridis* (Order: Anura) in Fars Province. – Unpublished MSc Dissertation. Shiraz University, Shiraz, Iran.
- BALLETTO, E., M. A. CHERCHI & J. GASPERETTI (1985): Amphibians of the Arabian Peninsula. – Fauna of Saudi Arabia, **7**: 318–392.
- BALOUCHE, M. & H. Q. KAMI (1995): Iran Amphibians. – Tehran University Press, No. 2250.
- BANCROFT, J. D. (1991): Theory and Practice of Histological Techniques. – Churchill Livingstone, New York, 726 pp.
- DUBOIS, A. & A. BOUR (2010): The nomenclatural status of the nomina of amphibians and reptiles created by Garsault (1764), with a parsimonious solution to an old nomenclatural problem regarding the genus *Bufo* (Amphibia, Anura), comments on the taxonomy of this genus, and comments on some nomina created by Laurenti (1768). – Zootaxa, **2447**: 1–52.
- EISELT, V. J. & W. J. F. SCHMIDTLER (1973): Froschlurche aus dem Iran unter Berücksichtigung außeriranischer Populationsgruppen. – Annalen des Naturhistorischen Museums in Wien, **77**: 181–243.
- FAKHARZADEH, F., J. DARVISH, H. G. KAMI, F. GHASEMZADEH & E. RASTEGAR-POUYANI (2014): New karyological and morphometric data on poorly known *Bufo surdus* and *Bufo luristanicus* in comparison with data of diploid green toads of the *Bufo viridis* complex from South of Iran. – Asian Herpetological Research, **5**: 168–178.
- FROST, D. R. (2014): Amphibian Species of the World: an Online Reference. Version 6.0. – American Museum of Natural History, New York, USA. Electronic Database available at <http://research.amnh.org/herpetology/amphibia/index.html>, accessed 15 February 2015.
- GOSNER, K. L. (1960): A simplified table for staging anuran embryos and larvae with notes on identification. – Journal of Herpetology, **16**: 183–190.
- GURR, E. (1962): Staining animal tissues—practice and theoretical, London Leonard Hill Limited, London, 631 pp.
- HADDAD, C. F. B. & C. P. A. PRADO (2005): Reproductive modes in frogs and their unexpected diversity in the Atlantic forest of Brazil. – BioScience, **55**: 207–207.
- IUCN (2014): The IUCN Red List of Threatened Species. – Available at <http://www.iucnredlist.org/details/54772/0>, accessed 03 February 2014.
- JAVARI, M. & F. TORKI (2009): Notes on morphology, ecology, behavior and systematic of *Bufo luristanicus* Schmidt, 1952 (Anura: Bufonidae). – Herpetozoa, **21**: 171–178.
- JENNINGS, R. D. & N. J. SCOTT (1993): Ecologically correlated morphological variation in tadpoles of the Leopard frog, *Rana chiricahuensis*. – Journal of Herpetology, **27**: 285–293.
- KHAN, M. S. & S. A. MUFTI (1994): Oral disc morphology of amphibian tadpole and its functional correlates. – Pakistanian Journal of Zoology, **26**: 25–30.
- MCDIARMID, W. & R. ALTIG (1999): Tadpoles: the biology of anuran larvae. – The University of Chicago Press, Chicago and London, 444 pp.
- NOKHBATOLFOGHAI, M. (2009): Developmental study of amphibians in Fars Province. – Shiraz University, Shiraz (Report).
- NOKHBATOLFOGHAI, M., J. R. DOWNIE, A. K. CLELLAND & K. RENNISON (2005): The surface ciliation of anuran amphibian embryos and early larvae: patterns, timing differences and functions. – Journal of Natural History, **39**: 887–929.
- NOKHBATOLFOGHAI, M. & J. R. DOWNIE (2005): Larval cement gland of frogs: comparative development and morphology. – Journal of Morphology, **263**: 270–283.
- NOKHBATOLFOGHAI, M. & J. R. DOWNIE (2007): Amphibian hatching gland cells: pattern and distribution in anurans. – Tissue and Cell, **39**: 225–240.
- NOKHBATOLFOGHAI, M. & J. R. DOWNIE (2008): The external gills of anuran amphibians: comparative morphology and ultrastructure. – Journal of Morphology, **269**: 1197–1213.
- ROUSHENAS, F. (2013): Impact of Sodium Arsenite (NAASO₂) on development of *Pseudepidalea viridis* (*Bufo viridis*). – Unpublished MSc Dissertation. Shiraz University, Shiraz, Iran.
- SCHMIDTLER, J. J. & J. F. SCHMIDTLER (1969): Über *Bufo surdus*; mit einem Schlüssel und Anmerkungen zu den übrigen Kröten Irans und West-Pakistans. – Salamandra, **5**: 113–123.
- SMITH, C. C. & S. D. FRETWELL (1974): The optimal balance between size and number of offspring. – American Naturalist, **108**: 499–506.
- STÖCK, M., R. GÜNTHER, & W. BÖHME (2001): Progress towards a taxonomic revision of the Asian *Bufo viridis* group: Current status of nominal taxa and unsolved problems (Amphibia: Anura: Bufonidae). – Zoologische Abhandlungen / Staatliches Museum für Tierkunde Dresden, **51**: 253–319.
- ZAREIAN, H., A. C. GHOLAMHOSSEINI, H. R. ESMAEILI & A. TEIMORI (2012): Vertebrates of Kuh-e-Gorm non-hunting area, Jahrom, Iran: Diversity, conservation and challenges. – Iranian Journal of Animal Biosystematics, **8**: 169–182.